Proceedings of the
International Conference on Mechanical Engineering 2007
(ICME2007) 29- 31 December 2007, Dhaka, Bangladesh

ICME07-AM-03

MEASUREMENT OF STRUCTURE-BORNE SOUND IN TRAPEZOIDAL CORRUGATED PLATES

Nirmal Kumar Mandal

Central Queensland University,
Bruce Highway, North Rockhampton,
Queensland 4702, Australia.

ABSTRACT

Structural intensity technique is used to measure vibration power flow in trapezoidal corrugated plates for flexural waves. The measurements are carried out in far-field conditions taking into account of cross-spectra of acceleration in the frequency domain. Two trapezoidal corrugated plates are used. To investigate the effects of rigidity on flexural wave power transmission and vibration levels, an isotropic plate is also considered for comparison. Method of elastic equivalence is used to model the elastic properties of the corrugated plates so as to apply the classical orthotropic plate theory. Multi-channel FFT analyzer is used for data acquisition such as input force and input acceleration signals, far-field acceleration driving point acceleration and coherence function between input force and far-field acceleration.

Keywords: Structural intensity, trapezoidal corrugated plate, far-field conditions.

1. INTRODUCTION

Machinery-induced vibrations are often a cause of concern or annoyance to orthotropic structures in buildings, ships and air-craft and vibration control is therefore a topic of continuing study. In any such problems, the first approach is usually to modify sources and isolate them from the surrounding structures via resilient vibration isolators. The vibration transmission characteristics of the structures between the sources and the area of unacceptable vibration levels must be examined and appropriate vibration control measures should be taken. It can be seen that from the vibration control point of view, there is a continuing interest in vibration isolation and structural vibration transmission.

Most of the previous works undertaken on vibration power flow (structural intensity) were related to simple structures, typically beams and plates in flexure using the analysis both in time domain and frequency domain [1-6].

Structural intensity can be computed numerically when predictions of structural behavior in various conditions are needed for complex build-up structures. Vibration intensity, generated by the interaction of dynamic stresses and vibration velocities, for beams and plates can be found by the finite element method [7-9], by statistical energy analysis [10]. The vibration power flow behaviors of a rectangular plate with stiffeners attached at various locations are investigated by Xu, et al. [11]. The effects of geometric properties of the stiffeners on power flow are quantified. It is shown that injected and transmitted vibration power is dependent on the natural frequency and flexural rigidity.

Using power flow technique, vibration wave power was also formulated to single-layer naturally orthotropic plates both for general [12] and far-field condition [13] using flexural wave and for general conditions [14] using quasi-longitudinal wave. In addition, the effects of flexural rigidity of different corrugated plates on damping loss factor were also quantified [15].

It is seen from the literature survey that not enough research has been undertaken relating to vibration power flow on orthotropic materials. Beam stiffened plates, plate grid structures, and corrugated plates are usually used in automotive, ship and aircraft structures. As this method gives a clear picture of locations of energy sources and sinks and quantifies energy transmission paths by employing vector maps, hence it essentially can be used for controlling noise and vibration in industry by incorporating proper damping treatments. Therefore an experimental study on trapezoidal corrugated plates using structural intensity is carried out to investigate the influences of flexural rigidity of the plates on vibration transmission and its response. Consequently the effectiveness of geometric modification (passive control method) of plates for vibration energy control is quantified.

2. INPUT POWER AND INTENSITY

The core of input power and vibration power flow was based on the imaginary part of the cross-spectrum of two signals: between force and acceleration signals at input point for input power and between two acceleration or velocity signals at the measurement locations on the structure for vibration power.

In the frequency domain, total active power injected through a point junction by a point force is obtained as [4]

$$P_i = \frac{1}{\omega}\mathrm{Im}\{G_{Fa}\} \quad (1)$$

where G_{Fa} is the cross-spectrum of force and acceleration signals, Im is the imaginary part, and $\omega\ (=2\pi f)$ is the angular frequency. The imaginary part of the cross-spectrum of equation (1) could be achieved from FFT analyzer and by post-processing using Matlab or MS Excel, the input power P_i (W) could be computed. The equation (1) is valid for both isotropic and orthotropic plates.

The idea of far-field power was first defined by Noiseux [1]. The far-field condition simplifies structural intensity estimation. In isotropic plates, two components of active power from shear force (P_s) and moment (P_M) are equal [1]. For isotropic plates, the far field power, also called time averaged power or active power, could be obtained as Linjama, et al. [4]

$$I = \frac{2\sqrt{Dm''}}{d\omega^2}\mathrm{Im}\{G_{12}\} \quad (2)$$

Where I is the intensity (far-field power) in the direction of the transducer pair from 2 to 1 as in figure 1, d is the spacing of the accelerometers, D is the flexural rigidity of the plate, m'' is the mass per unit area of the plate, G_{12} is the cross-spectrum of acceleration signals, Im{} is the imaginary part. The equation (2) is applicable both in x and y directions of the plate (figure 1).

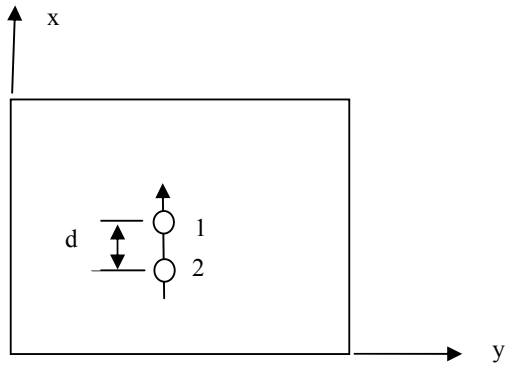

Fig 1: Co-ordinate system of plate along with two-point transducer array.

By normalizing the power flow at the far field conditions with respect to input power at a point source, power ratio, R, for the two transducer method could be found by taking the ratio of equation (2) to (1)

$$R = \frac{2\sqrt{Dm''}}{d\omega}\frac{\mathrm{Im}\{G_{12}\}}{\mathrm{Im}\{G_{Fa}\}} \quad (3)$$

The flexural wave power in naturally orthotropic plates can be obtained using finite difference approximation. Recently, a measurement method to quantify power flow in naturally orthotropic plates has been developed [13]. This model is indicating power transmission in x-direction of the plate and is presented below as

$$I_x(f) = \frac{2\sqrt{D_x m''}}{d\omega^2}\mathrm{Im}\{G_{12}\} \quad (4)$$

where D_x is the flexural rigidity of the plate in x-direction. This relation presents the flow of vibration power in orthotropic plates in the x direction from point 2 to 1 (figure 1). The y-component of this power could be obtained by interchanging the x and y axes in the equation (4).

3. EXPERIEMENTS

The objective of this experiment is to measure vibration power transmission in technically orthotropic plates. Trapezoidal corrugated plates, one small and one big, are considered. In addition, one isotropic plate of steel is also used for investigating the effect of flexural rigidity on power transmission. The method of elastic equivalence [16 - 17] is used to replace the structurally orthotropic plate with the equivalent naturally orthotropic plate of uniform thickness. Figure 2 shows a typical repeating section of corrugated plate.

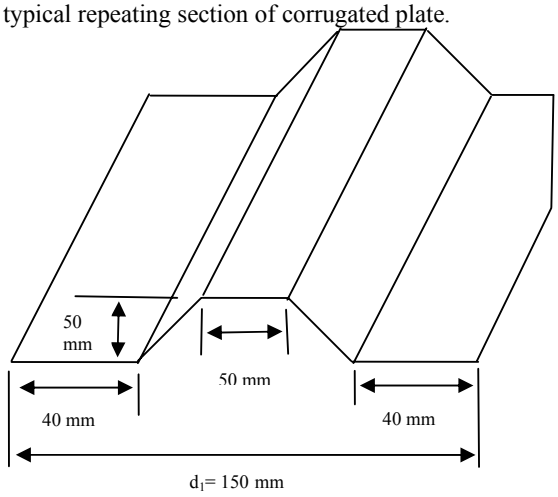

Figure 2: One repeating section of trapezoidal corrugated plate.

A laboratory test rig was constructed for experiments. The schematic diagram and instrumentation for the measurement of flexural wave power on a steel isotropic plate and trapezoidal corrugated plates were fabricated as in figure 3. At the upper end of the plate, a mini-shaker (B&K type 4810) was used to provide random white noise excitation to the plates through a force transducer (B&K type 8200). Two accelerometers mounted away from the source and boundaries were used to measure far-field power. The major components of instrumentation were the miniature accelerometers (piezoelectric, ICP, with an effective mass of 1.7 gm) and a multi-channel FFT analyzer (HP 35670A). The accelerometers were mounted on the plate with beeswax. The mini-shaker was driven by internal noise source of the FFT analyzer.

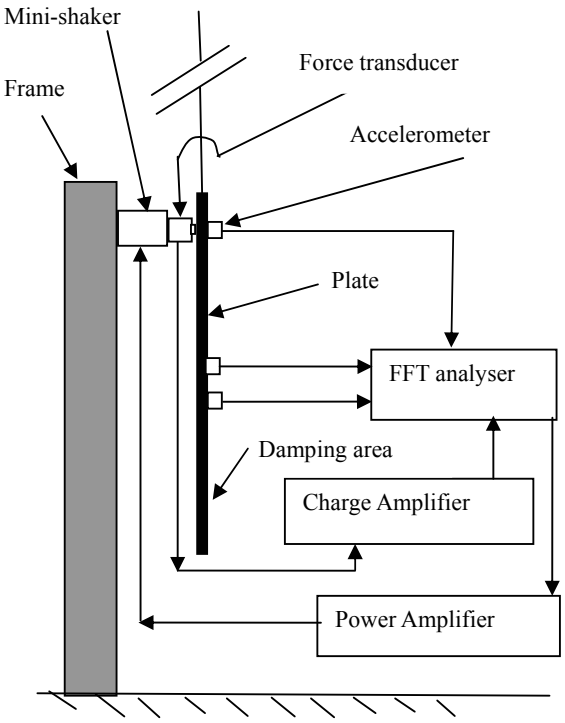

Fig 3: Test rig and instrumentation of a freely suspended plate.

The sides of all plates (figure 4) are 0.90 m and the thickness of the isotropic plate and equivalent corrugated plates is 0.8 mm. The material properties such as Young's modulus and Poisson's ratio are 162.8 GPa and 0.31 respectively. With these plate dimensions and material properties, it can be expected that the far-field condition (at least half a wavelength from the boundaries and source) is at the center of the plate at frequencies from about 9.12 Hz upwards. The upper frequency limit for flexural wave condition to be valid (wavelength equal to six times the thickness of the plate [18] was 320.7 kHz. The spacing of the accelerometer positions should be as short as possible so as to minimize finite difference error, but too short a distance causes phase mismatch error. The spacing, d, was chosen rather arbitrarily to be 20 mm. The spectral bandwidth was set at 800 Hz. At the upper frequency limit of 800 Hz, the wavelength was calculated to be 96.10 mm for isotropic plate (IP). For small trapezoidal corrugated plate (STCP) and big trapezoidal corrugated plate (BTCP) the flexural wavelengths are respectively 520.34 mm and 931.06 mm. Thus the accelerometer spacing is approximately 1/4.8 of the wave length for IP, 1/26 for STCP and 1/46 for BTCP

Suspension of trapezoidal corrugated plates needs careful attention so as to make x-axis parallel to the direction of corrugation (figure 2). As a result the flexural rigidity in x-direction of the plates, D_x, is greater than that of D_y. In every plate, like isotropic, two measurement lines were considered where different points were located as shown in figure 4. Only a small change was made for the measurement of energy transfer in the big trapezoidal corrugated plate. This was due to its different characteristic dimension d_1.

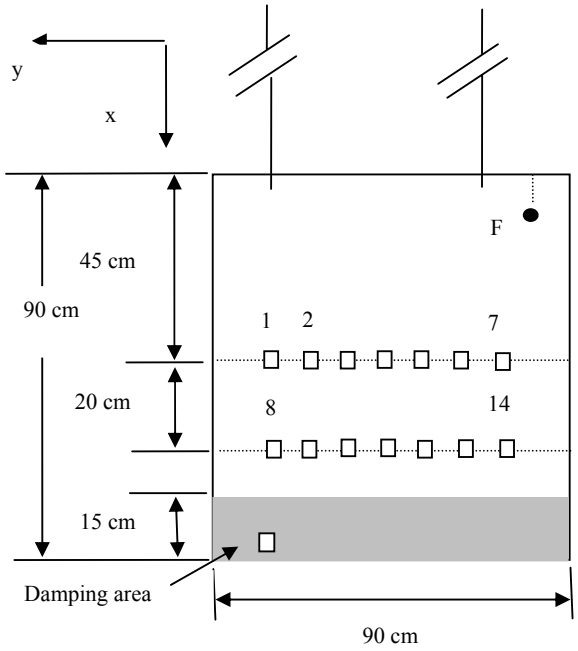

Fig 4: Different measurement points on two measuring lines (seven on each line), indicating locations of applied force and damping on plate.

In the measurements, mainly the imaginary part of cross-spectrum between two accelerometers' signals at the far-field (as required by equation 4) and the same between force and acceleration at the excitation point (as required by equation 1) was measured. The mini-shaker, providing random white noise, was connected to the internal noise source of the FFT analyzer. White noise commonly known as random excitation is constant in magnitude over the frequency range. For the measurements of cross-spectrum between two acceleration signals for all fourteen points in the far fields (figure 4), a fixed array of transducers (two accelerometers at a 'd' distance apart, figure 1) was used for all points rather than moving a transducer sequentially between the locations of the accelerometer for measurement point. In the case of one transducer arrangement, a stationary field should be made during data acquisition of cross-spectral. Additional transducer for two-transducer measurement exerts a negligible local disturbance as the mass of the transducer is small. Investigation of the local influence on vibration field is beyond the scope of this paper. The FFT analyzer was used to collect 200 ensemble averages of the cross-spectra, auto-spectra and coherence functions needed in the subsequent processing.

An example of coherence functions observed during data acquisitions in steel STCP is shown in figure 6 with the frequency resolution of 8 Hz. Some lack of coherence occurred at the low frequencies and it was deemed to be acceptable on overall basis [4]. A more sufficient spectral resolution may improve coherence values at these frequencies.

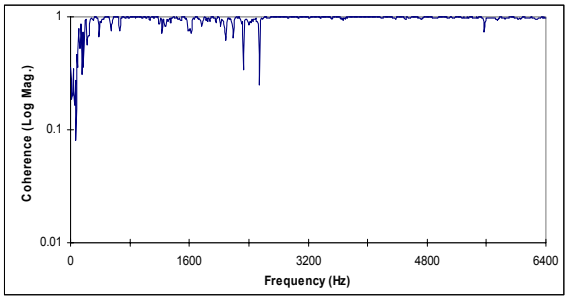

Fig 5: Coherence function between force and acceleration at input point for STCP, resolution of 8 Hz.

3.1 Results

In this study, both input power and far-field power of the plates were measured. The same force signal was applied throughout the experiments for all plates. This enables a comparison of far-field power between isotropic plates and corrugated plates to investigate the influence of flexural rigidity on power transmission. For flexural wave power measurement, input force was injected to a point (figure 4) on the plates in the direction perpendicular to the plates. The location of input force was chosen at the top corner of the plate so as to observe more intensity field at distinct frequencies of resonant and non-resonant character. The excitation force signal was random white noise, given by the internal noise source of the FFT analyzer used, in the frequency range of 0 Hz to 800 Hz as in the figure 6. A stable constant magnitude of force (N) is observed throughout the frequency range.

Input power and far-field power for an isotropic plate and both for small and big trapezoidal corrugated plates were estimated. The far-field power was normalized to input power to facilitate comparison of the results and the method. This is possible because the same measurement state of input force was used for all plates to ensure a constant and repeatable condition.

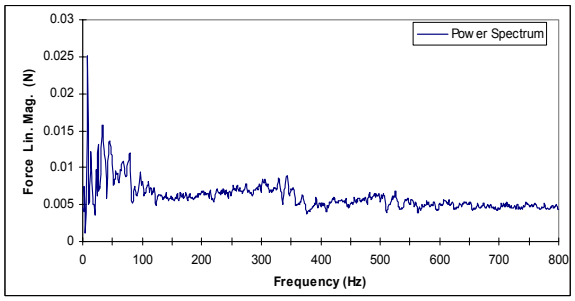

Fig 6: Random force signal for low frequency range measured by force transducer.

For STCP, figures 7 - 9 show normalized far-field power to input power. For BTCP, on the other hand, the same method was used for data acquisition and analysis. Spectral resolution was increased to 4 Hz for calculation of energy transfer. The reason for higher spectral resolution is because different resolution lines of 200 were considered to make it different from that of STCP.

Figure 10 shows normalized far-field power to input power for this plate.

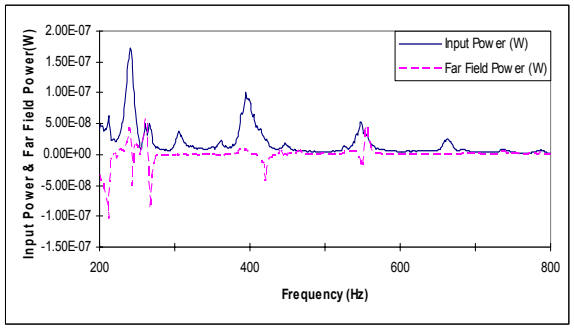

Fig 7: Normalized far-field power and input power for STCP from upper measurement line, spectral resolution of 1 Hz.

4. DISCUSSION

4.1 Measurement of Structural Intensity

The standard way of providing soundness of structural intensity technique is to normalize vibration power transmission to input power [4, 5, and 19]. Under all conditions, it is expected that input power must be greater than the vibration power flow [4] for identical conditions on the same structure.

From figures 7 and 9, it is observed that input power has mostly higher values than those of far-field power for STCP. This is confirmed by figure 8 where power transmission is plotted in ratio form (far-field to input). In some cases, far-field power may however exceed the input power and power ratio between far-field power and input power on the same plate is greater than unity [4-5].

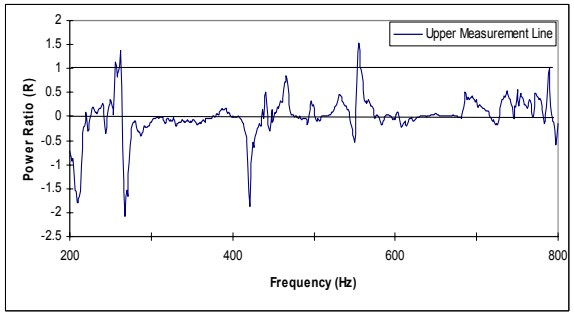

Fig 8: Power ratio of far-field power and input power for STCP, spectral resolution of 1 Hz.

In figure 10, for BTCP, a similar pattern of power flow transmission is observed. It is further important to note that in some frequencies, negative values of far-field power were detected (figures 7, 9 and 10) and thereby power ratio became negative. However, the characteristics of the results are consistent with the results reported in the literature [4-5].

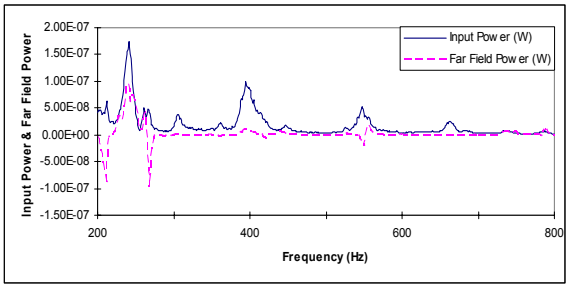

Fig 9: Normalized far-field power and input power for STCP from lower measurement line, spectral resolution of 1 Hz.

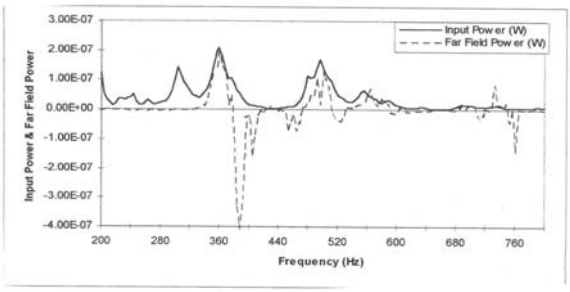

Fig 10: Normalized far-field power to input power for BTCP from upper measurement line, spectral resolution of 4 Hz.

These two aspects of vibration power flow may be explained by the following idea. Three types of power flow pattern [20] are observed: straight type, S-shaped type and vortex type. Among them, S-shaped type and vortex type flow pattern may play important roles for energy transfer, causing negative energy flow.

There are seven measurement points on each line grid. Using a few more measurement points on each line and averaging the vibration power crossing through these points may solve the problem of less input power than that of far-field power at some frequencies. A consideration of less measurement points on a line results in a loss of valuable frequency components. However, this is a usual practice for plate vibration measurement [4].

In addition, reflections and scatterings of waves from edges of the plates (only the lower side of the plates is damped) and rotational (vortex) characteristics of power flow field create additional influence on far-field power which can cause it to be greater than input power and yielding negative values.

4.2 Passive Controlling Method

In this research, both vibration power and vibration amplitude of corrugated plates are compared with that of the isotropic plate (figures 11). From this figure, it is shown that vibration power flow is reduced in corrugated plate in comparison to that of isotropic plate. The value of flexural rigidity for isotropic plate (7.684 N-m) was less than the rigidities of corrugated plates (7922.93 N-m for STCP and 97.76×10^3 N-m for BTCP). It is observed that with the increase of flexural rigidity, vibration power flow reduces. This outcome is supported by the results of the graph of figure 12. Frequency response function (FRF) of acceleration of STCP and BTCP is reduced to that of the isotropic plate. Higher stiffness enhances more damping, thereby amplitude of vibration reduces (figure 12) and structural intensity does too (figures 7 and 9). Only for a few frequencies the vibration response of isotropic plate is less than that of corrugated plates (figure 12) and the ratio of FRFs (trapezoidal to isotropic plate) greater than unity. This is because of resonance vibration responses of the corrugated plates; vibration response at resonance is larger compared to that of other frequencies and it can be greater than the response of isotropic plate. However, on an overall basis, it may be argued that vibration responses are reduced for corrugated plates.

A passive method of controlling energy transfer by increasing flexural rigidity of the structures gives a better way of control not only to reduce vibration amplitude but also to reduce vibration energy transfer. As higher rigidity of plates ensures more damping, more vibration energy is absorbed in the plates resulting in less acoustic power radiation to the surroundings. The increase of flexural rigidity by corrugation of the plates does not result in any major increase in mass of the plate. To achieve the same amount of stiffness increase by increasing thickness of the plate or stiffening with other beams would surely yield more mass of the plate. Corrugation of plate is therefore an effective controlling method of vibration power and vibration amplitude for flexural waves. Effects on rigidity of sinusoidal and other types of corrugation require more attention now to investigate its influence on vibration energy transfer by flexural waves and in-plane waves.

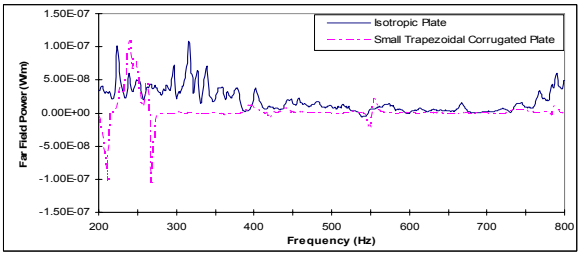

Fig 11: Comparison of far-field power for isotropic plate (IP) and STCP from lower measurement line.

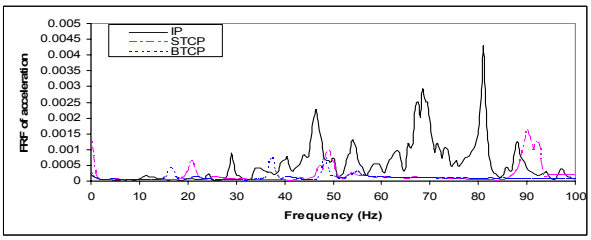

Fig 12: Comparison of frequency response function (FRF) of acceleration of isotropic plate (IP), STCP, and BTCP, spectral resolution of 1 Hz.

5. CONCLUSIONS

An experimental investigation is carried out to find the effects of flexural rigidity on flexural wave power flow and vibration response. It is observed that due to the increase of flexural rigidity, both vibration power flow and amplitude are reduced. As a result, it may be argued that the structural design, increasing the flexural rigidity by modifying its geometry, is an effective passive method for noise and vibration control in industries. Increase of rigidity by corrugation does not yield much weight penalty as compared to other methods. In addition, increasing rigidity does not require sensors/actuators necessary for active vibration controls.

6. REFERENCES:

1. Noiseux, D. U., 1970, "Measurement of power flow in uniform beams and plates", Journal of the Acoustical Society of America, 47: 238-247.
2. Pavic, G., 1976, "Measurement of structure borne wave intensity, part I: Formulation of the methods", Journal of Sound and Vibration, 49: 221-230.
3. Verheij, J. W., 1980, "Cross-spectral density methods for measuring structure borne power flow on beams and pipes", Journal of Sound and Vibration, 70: 133-138.
4. Linjama, J. and Lahti, T., 1992, "Estimation of bending wave intensity in beams using the frequency response technique", Journal of Sound and Vibration, 153: 21-36.
5. Bauman, P. D., 1994, "Analytical and experimental evaluation of various techniques for the case of flexural waves in one-dimensional structures", Journal of Sound and Vibration, 174: 677-694.
6. Arruda, J. R. F. and Campos, J. P., 1996, "Experimental determination of flexural power flow in beams using a modified prony method", Journal of Sound and Vibration, 197: 309-328.
7. Gavric, L. and Pavic, G., 1993, "A finite element method for computation of structural intensity by the normal mode approach", Journal of Sound and Vibration, 164: 29-43.
8. Hambric, S. A. and Taylor, P. D., 1994, "Comparison of experimental and finite element structure-borne flexural wave power measurements for straight beam", Journal of Sound and Vibration, 170: 595-605.
9. Hambric, S.A., 1995, "Comparison of finite element prediction and experimental measurements of structure-borne power in a T-shaped beam", Proc. Inter-noise 95, pp. 685-688.
10. Langley, R. S., 1992, "A wave intensity technique for the analysis of high frequency vibration", Journal of Sound and vibration, 159: 483-502.
11. Xu, X. D., Lee, H. P. and Lu, C., 2005, "Power flow paths in stiffened plates", Journal of Sound and Vibration, 282: 1264-1272.
12. Mandal, N. K., Rahman, R. Abd. and Leong, M. S., 2003, "Structure-borne power transmission in thin naturally orthotropic plates: general case", Journal of Vibration and Control, 9: 1189-1199.
13. Mandal, N. K., Rahman, R. Abd. and Leong, M. S., 2002, "Prediction of Structure borne sound in orthotropic plates for far field conditions", Journal of Vibration and Control, 8: 3-12.
14. Mandal, N. K., Leong, M. S. and Rahman R. Abd., 2000, "Measurement of quasi-longitudinal wave power in thin single-layer naturally orthotropic plates", International Journal of Acoustics and Vibration, 5: 106-108.
15. Mandal, N. K., Rahman, R. Abd. and Leong, M. S., 2004, "Determination of damping loss factors of corrugated plates by the half–power bandwidth method", Ocean Engineering: an International Journal of Research and Development, 31: 1313-1323.
16. Troitskey, M. S., 1976, *Stiffened Plates: Bending, Stability and Vibration*, Elsevier, Amsterdam.
17. Ugural, A. C., 1981, Stress *in plates and shells*, New York: McGrawHill.
18. Cremer, L. and Heckl, M., 1988, *Structure-Borne Sound: Structural Vibration and Sound Radiation at Audio Frequencies*, Springer-Verlag, Berlin.
19. Mandal, N. K., Rahman, R. Abd. and Leong, M. S., 2005, "Experimental Investigation of Vibration Power Flow in Thin Technical Orthotropic Plates by the Method of Vibration Intensity", Journal. Sound and Vibration, 285: 669-695.
20. Tanaka, N., 1996, "Vibration and acoustic power flow of an actively control thin plate", Noise Control Engineering Journal, 44: 23-33.